Suplemento de la Revista Mexicana de Física **3** 0308027 (2022) 1–5

Coherent neutral pion and eta meson photoproduction on the deuteron

T. Ishikawa, H. Fujimura, H. Fukasawa, R. Hashimoto, Q. He, Y. Honda, S. Kaida, J. Kasagi, S. Kuwasaki, M. Miyabe, F. Miyahara, K. Mochizuki, N. Muramatsu, A. Nakamura, K. Nawa, S. Ogushi, Y. Okada, K. Okamura, Y. Onodera, M. Sato, H. Shimizu, H. Sugai, K. Suzuki, S. Takahashi, Y. Taniguchi, Y. Tsuchikawa, H. Yamazaki, and R. Yamazaki

Research Center for Electron Photon Science (ELPH), Tohoku University, Sendai 982-0826, Japan

T. Iwata, Y. Tajima, and H.Y. Yoshida

Department of Physics, Yamagata University, Yamagata 990-8560, Japan.

A. Kawano, and Y. Sakamoto

Department of Information Science, Tohoku Gakuin University, Sendai 981-3193, Japan.

K. Maeda

Department of Physics, Tohoku University, Sendai 980-8578, Japan.

S. Masumoto, and Y. Obara

Department of Physics, University of Tokyo, Tokyo 113-0033, Japan.

K. Ozawa

Institute of Particle and Nuclear Studies (IPNS),
High Energy Accelerator Research Organization (KEK), Tsukuba 305-0801, Japan.

Received 13 January 2022; accepted 18 February2022

Measurements of the cross sections are conducted for coherent photoproduction of the neutral pion and eta meson on the deuteron, $\gamma d \to \pi^0 \eta d$, at the incident energy in the range of the reaction threshold to 1.15 GeV. A rapidly increasing trend below 1 GeV is observed in the total cross section. The data are effectively reproduced by theoretical calculations incorporating the meson-deuteron final-state interactions. However, the measured deuteron angular distribution $d\sigma/d\Omega_d$ in the center-of-mass frame (γd) is rather flat, and it differs significantly from the strong backward-peaking behavior expected in the kinematics of deuteron formation after $\pi^0\eta$ photoproduction on an initial bound nucleon. In addition, the $d\sigma/dM_{\eta d}$ differential cross section exhibits a prominent enhancement near the ηd threshold, while $d\sigma/dM_{\pi d}$ exhibits an enhancement near the known πd resonance with $I = 1$ and $J^P = 2^+$. From these observations, we have concluded that two reaction sequences occur; $\gamma d \to \pi^0 \mathcal{D}_{01} \to \pi^0 \eta d$ and $\eta \mathcal{D}_{12} \to \pi^0 \eta d$, where $\mathcal{D}_{IJ}$ denotes a state with a baryon number of 2, an isospin I, and a spin J. The enhancement corresponding to $\mathcal{D}_{01}$ is expected to be a theoretically predicted ηNN bound state with $I = 0$ and $J^P = 1^-$ or a virtual state of ηd. It is found that attraction between ηd is certainly very strong.

Keywords: Coherent meson photoproduction; ηd threshold structure.

DOI: https://doi.org/10.31349/SuplRevMexFis.3.0308027

1. Introduction

Although a meson serves as the glue that binds nucleons within a nucleus, it is not considered to become a constituent of the nucleus. The E15 experiment at J-PARC recently provided evidence for the so-called K^-pp state where K^- becomes a constituent of the nucleus [1, 2]. The existence of the hyperon resonance $\Lambda(1405)1/2^-$, or a K^-p bound state, facilitates K^-pp formation. In addition, the eta meson (η) and nucleon have strong attractive forces, thereby forming the nucleon resonance $N(1535)1/2^-$ that is the lowest-lying negative-parity nucleon resonance, and thus it is considered as a nucleon chiral partner. Furthermore, η is also expected to be a constituent of some nucleus. Over five decades ago, Haider and Liu predicted an exotic η-mesic nucleus that is a η-nucleus quasi-bound state formed solely by the strong force [3]. The η-mesic nucleus enables us to investigate the behavior of η and/or $N(1535)1/2^-$ in a dense nuclear environment [4–10].

The lightest η-mesic nucleus is possibly an ηd bound state, which is expected to be a mixing state with $I = 0$ and $J^P = 1^-$ between the S-wave ηd system and the S-wave N and $N(1535)1/2^-$ molecule-like system. Ueda conducted a three-body isoscalar ηNN-πNN coupled-channel calculation, and predicted an isoscalar ηNN bound state near the sum of ηd masses with $\Gamma = 0.01$–0.02 GeV [11, 12]. In ηd production from the pn collision, a significant deviation was observed over the phase space near the threshold [13–17]. This deviation could correspond to the predicted state although it did not provide the mass and width of the ηd system.

We have attempted to find the ηd bound state in photoproduction. A GeV photon beam produces baryon resonances from the nucleon. The excitation spectrum itself is an important testbed for understanding the non-perturbative domain of the quantum chromodynamics. Baryon resonances are likely to be generated by the quasi-free (QF) nucleon even when a nuclear target is irradiated with the photon beam. The QF nu-

cleon, or the excited baryon resonance, is a participant, while the residual nucleus becomes a spectator. No spectator exists in coherent photoproduction of a meson or several mesons where the same nucleus appears both in the initial and final states. Therefore, a meson-nucleus system is expected to be produced in coherent meson photoproduction.

However, there is no indication of the ηd bound state in $\gamma d \to \eta d$ [18, 19]. The η angular distributions in the reaction are expressed by the coherent sum of the elementary $\gamma N \to \eta N$ amplitudes. Owing to the kinematics for deuteron formation in the final state, the deuteron angular distribution is strongly backward peaking in the center-of-mass (CM) frame (γd). Coherent photoproduction of a single neutral meson is governed by the coherent sum of the elementary amplitudes and nuclear form factor. By contrast, the same is not true for coherent photoproduction of two neutral mesons.

Deuteron emission shows rather flat angular distributions in the CM frame for $\gamma d \to \pi^0\pi^0 d$. Therefore, QF $\pi^0\pi^0$ production with deuteron coalescence is ruled out; alternatively, a reaction sequence $\gamma d \to \mathcal{D}_{0\mathrm{J}} \to \pi^0\mathcal{D}_{1J'} \to \pi^0\pi^0 d$ process is dominant, where $\mathcal{D}_{IJ}$ denotes some two-baryon state with isospin I and spin J [20, 21]. In $\gamma d \to \pi^0\eta d$, two reaction sequences are expected: $\gamma d \to \mathcal{D}_{1J} \to \pi^0\mathcal{D}_{0J'} \to \pi^0\eta d$ and $\gamma d \to \mathcal{D}_{1J} \to \eta\mathcal{D}_{1J'} \to \pi^0\eta d$. Note that the different states are described by the same symbol $\mathcal{D}_{1J}$, $\mathcal{D}_{0J'}$, or $\mathcal{D}_{1J'}$. A low relative momentum condition between ηd can be given in $\gamma d \to \pi^0\eta d$, where a possible ηd bound state is likely to be produced, and its tail may appear in $\mathcal{D}_{\mathrm{IS}}$. In this proceeding, we report the ηd threshold structure that appears in $\gamma d \to \pi^0\eta d$. Further details are provided elsewhere [22].

2. Experiment

We conducted eight series of experiments aiming at baryon spectroscopy by means of meson photoproduction [23] at the Research Center for Electron Photon Science (ELPH), Tohoku University, Japan [24]. We generated bremsstrahlung photons as a photon beam [25] by moving a radiator made up of a carbon thread directly into the stored 1.2-GeV electrons in a synchrotron [26]. To determine the energy of a produced photon, we detected the corresponding recoil electron with a set of counters for photon tagging, STB-Tagger II [25]. The typical tagging rate was 20 MHz, and the tagged photon energy was in the range of 0.75 to 1.15 GeV, corresponding to the γd CM energies in the range of 2.50 to 2.80 GeV. We monitored the photon beam profile, or the (x, y) intensity map at the target location regularly [27]. The horizontal and vertical widths of the photon beam were ≈ 7 and ≈ 8 mm (σ), respectively. The horizontal positions are correlated with the horizontal components of the incident photon momentum [29]. The size and correlation of the photon beam were considered for estimating the acceptance of detecting the $\pi^0\eta d$ final-state events. The photon transmittance, or the probability of finding a photon arriving at the target location when an electron is detected with STB-Tagger II, was also monitored regularly [28]. The photon transmittance was $\approx 53\%$ on average.

We used a 45.9-mm-thick liquid deuterium target [30]. We measured the kinematic variables for all the generated final-state particles of $\gamma d \to \pi^0\eta d \to \gamma\gamma\gamma\gamma d$ using the FOREST detector with three different electromagnetic calorimeters (EMCs) [31]: 192 pure cesium-iodide crystals (CsI), 252 lead and scintillating-fiber sandwich modules (Lead/SciFi), and 62 SF5 and SF6 lead-glass counters (LG). The energy resolutions of CsI, Lead/SciFi, and LG are $\approx 3\%$, $\approx 7\%$, and $\approx 5\%$, respectively, for 1-GeV photons. We obtained the energy resolutions depending on the incident energy also at ELPH by using momentum-analyzed 0.1–0.8 GeV/c positron beams [32]. To identify charged particles, a hodoscope consisting of plastic scintillator sheets (PSH) was located before each EMC. We also investigated the position-dependent energy and time responses in detail for these PSHs by using the positron beams. The forward PSH was comprised of left-handed and right-handed spiral-shaped plastic scintillator sheets, having three layers in total, and it could provide the impact position of a charged particle. The trigger for the data acquisition (DAQ) required that multiple particles were detected together with a coincident photon-tagging signal [20, 21, 31, 33]. The trigger rate was ≈ 1.7 kHz and the DAQ effciency was $\approx 79\%$, on average.

3. Analysis

We selected the $\pi^0\eta d$ final-state events ($\gamma d \to \pi^0\eta d \to \gamma\gamma\gamma\gamma d$). We scanned the events including four EMC clusters without PSH hits, and a PSH hit. An EMC cluster without a corresponding PSH hit was recognized as a neutral particle, whereas a PSH hit was recognized as a charged particle regardless of whether the corresponding EMC cluster had a hit or not. We required that the time difference was less than three times that expected from the time resolution for every two out of four neutral EMC clusters. We analyzed the events that the charged particle was incident on the forward PSH, and that the PSH hit was delayed more than 1 ns with respect to the four neutral clusters. In addition, we required that a charged particle deposited an energy in PSH larger than two times that the minimum ionizing particle did.

We applied a six-constraint (6C) kinematic fit (KF) with the $\gamma d \to \pi^0\eta d$ hypothesis (CKF): the four-momentum conservation (4C), the two sets of the two-photon invariant masses being the π^0 and η masses (2C), respectively. In each event, we selected the most probable combination to divide four photons into two sets of the two photons from the π^0 and η decays. We calculated the momentum from the time delay for the charged particle under the condition that it had the deuteron mass. To reduce the contribution from other background reactions, we selected the events in which the χ^2 probability was higher than 0.2. The QF $\gamma p' \to \pi^0\eta p$ reaction is the most competitive background when the deuteron is misidentified as the proton. Therefore, we additionally re-

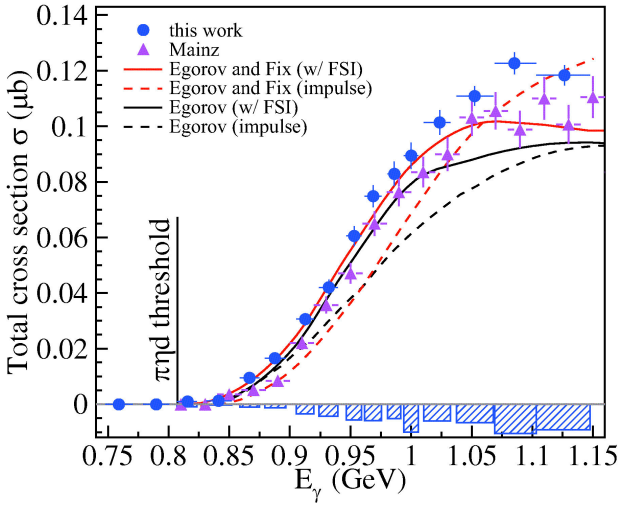

FIGURE 1. σ as a function of E_γ. The blue circles show σ obtained in this study, and the magenta triangles represent those obtained in Ref. [37] (Mainz MAMI). In each data point, the E_γ coverage is given by the horizontal error, whereas the statistical error of σ is shown by the vertical error. The dashed curves represent the calculations for the impulse terms, and the solid show those with FSIs. The red and black curves are taken from Ref. [38] and Ref. [39], respectively. The systematic errors of σ are shown in the hatched histograms.

quired the events so that χ^2 probability in another KF was lower than 0.01 for the $\gamma p' \to \pi^0\eta p$ hypothesis (QFKF). In this QFKF, we assumed that each component in the Cartesian coordinate of the initial proton momentum was measured as 0 MeV/c with a resolution of 40 MeV/c. We obtained the total energy of the proton by assuming that the spectator neutron was always on-shell. Finally, we carried out sideband-background subtraction to remove the accidental-coincidence events between detections in STB-Tagger II and FOREST.

4. Results

Figure 1 shows the total cross section σ as a function of the incident energy E_γ. We estimated the acceptance for detecting four photons and a deuteron through a Geant4-based [34–36] Monte-Carlo simulation. We modified the event generation from the phase space in order to reproduce the following kinematic variables: $M_{\eta d}$ (ηd invariant mass), $M_{\pi d}$ ($\pi^0 d$ invariant mass), and $\cos\theta_d$ (deuteron emission angle in the γd-CM frame). Note that $M_{\pi\eta}$ ($\pi^0\eta$ invariant mass) is directly obtained from $M_{\eta d}$ and $M_{\pi^0 d}$ at a fixed E_γ. The data obtained in this study agree with the previously obtained data at another facility, Mainz MAMI [37], within errors. We compared the data with existing theoretical calculations without (impulse terms only) and with final-state interactions (FSIs). The red curves represent the calculations in Ref. [38] (by Egorov and Fix), and the black in Ref. [39] (by Egorov), while the solid curves represent the calculation for the impulse terms, and the dashed represent those with FSIs.

As shown in Fig. 2, we obtained the three kinds of differential cross sections, $d\sigma/d\Omega_d$, $d\sigma/dM_{\eta d}$, and $d\sigma/dM_{\pi d}$, at E_γ = 1.01–1.15 and 0.95–1.01 GeV, The experimental data are shown by the blue circles with statistical errors, and the systematic uncertainties are represented by the hatched histogram. The experimentally obtained $d\sigma/d\Omega_d$ exhibits a gradually decreasing trend as $\cos\theta_d$ increases, similar to the $\gamma d \to \pi^0\pi^0 d$ reaction, suggesting that a reaction sequence occurs. An enhancement in $d\sigma/dM_{\eta d}$ is observed in the low-

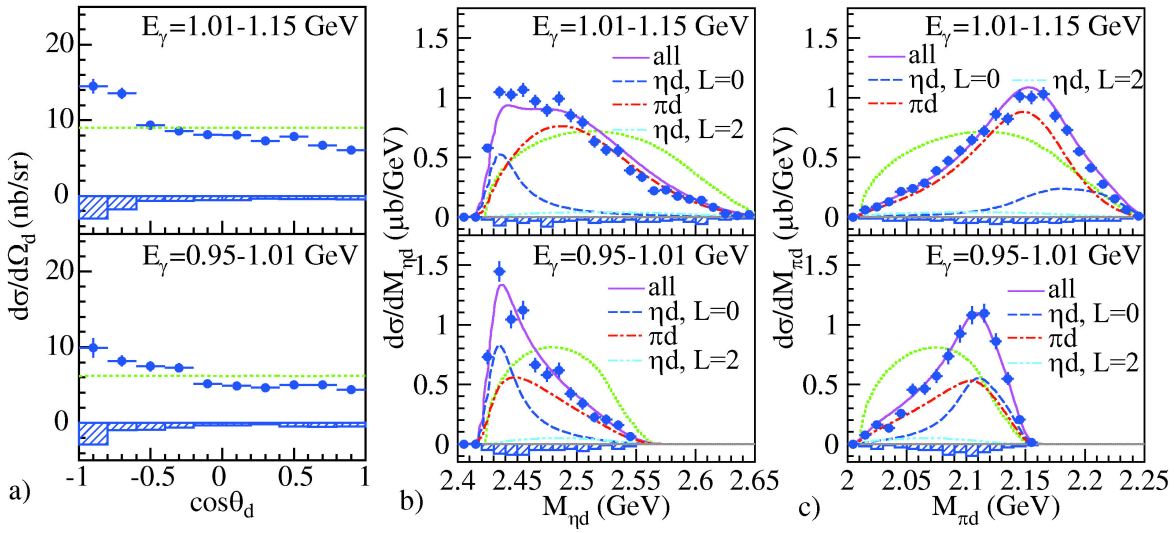

FIGURE 2. a) $d\sigma/d\Omega_d$, b) $d\sigma/dM_{\eta d}$, and c) $d\sigma/dM_{\pi d}$ at $E_\gamma = 1.01 - 1.15$ GeV (top) and $0.95 - 1.01$ GeV (bottom). The measured values are plotted by the blue circles, and their systematic errors are represented by the lower hatched histograms. The green dotted curves are the phase-space contributions, where the yields are normalized so as to reproduce the measured σ. In panels b) and c), the magenta solid curves represent the fitted function including S- (blue dashed) and D-wave (cyan two-dotted-dashed) decay contributions of $\mathcal{D}_{01}$, as well as a contribution from $\mathcal{D}_{12}$ (red dotted-dashed).

mass region as compared with the phase-space contribution. The observed enhancement is much wider at $E_\gamma = 1.01$–1.15 GeV than at $E_\gamma = 0.95$–1.01 GeV. In $d\sigma/dM_{\pi d}$, we observe a significant enhancement at high masses, which corresponds to the known πd resonance $\mathcal{D}_{12}$ with $I = 1$, $J^\pi = 2^+$, $M \simeq 2.14$ GeV, and $\Gamma \simeq 0.09$ GeV [21]. This resonance is the source of the broadening of the threshold enhancement in the ηd channel.

Only the ηd system in the S-wave with $I = 0$ and $J^P = 1^-$ ($\mathcal{D}_{01}$) contributes toward the peak formation in the vicinity of the threshold in $d\sigma/dM_{\eta d}$. We decomposed $d\sigma/dM_{\eta d}$ and $d\sigma/dM_{\pi d}$ into $\pi^0\mathcal{D}_{01}$ and $\eta\mathcal{D}_{12}$ contributions. Here, the $\mathcal{D}_{01} \to \eta d$ decay was assumed to occur in the S and D waves. In addition, we assumed that the mass distribution of $\mathcal{D}_{12}$ takes a Breit-Wigner shape, and that of $\mathcal{D}_{01}$ was expressed by a Flatté parameterization where the opening of the ηd channel was incorporated and the width Γ was given by $\Gamma = \Gamma_0 + g p_\eta c$ with the coupling g to the ηd channel, the width Γ_0 for the other open channels such as NN, πNN, $\pi\pi NN$, and $\pi\pi d$ and the momentum p of η in the rest frame of ηd. We performed a simultaneous fit the Breit-Wigner shape for $\mathcal{D}_{12}$ and Flatté parameterization for $\mathcal{D}_{01}$ to the mass distributions ($d\sigma/dM_{\eta d}$ and $d\sigma/dM_{\pi d}$) at $E_\gamma = 1.01$–1.15 and 0.95–1.01 GeV. The free parameters in this fit were M and Γ for $\mathcal{D}_{12}$, and M, Γ_0, and g for $\mathcal{D}_{01}$, and the yield ratio between the $\pi^0\mathcal{D}_{01}$ and $\eta\mathcal{D}_{12}$ contributions. The obtained parameters in the fit were $(M, \Gamma_0, g) = \left(2.427^{-0.006}_{+0.013}\ \text{GeV}, 0.029^{+0.006}_{-0.029}\ \text{GeV}, 0.00^{+0.41}_{-0.00}\right)$ for $\mathcal{D}_{01}$, and $(M, \Gamma) = \left(2.158^{-0.003}_{+0.003}, 0.116^{+0.005}_{-0.011}\right)$ GeV for $\mathcal{D}_{12}$. The S- and D-wave decay contributions of $\mathcal{D}_{01}$ together with the $\mathcal{D}_{12}$ contribution are also plotted in Fig. 2.

Prominent peaks are deduced in the vicinity of the ηd threshold in $d\sigma/dM_{\eta d}$, as shown in Fig. 2b). This threshold enhancement would correspond to the bound state of ηd predicted by Ueda [11, 12] or interpreted as a virtual state of ηd [40–42]. The former and latter cases result in a large Γ_0 and small g condition, and a small Γ_0 and large g condition, respectively. As both the fitted Γ_0 and g include 0 within the errors, we cannot determine whether the peak is a bound or virtual state. Attraction between ηd is certainly very strong.

5. Summary

We measured the cross sections for $\gamma d \to \pi^0\eta d$. The total cross section σ was found to show a significant enhancement near the threshold compared to the existing theoretical calculations for the impulse terms. The σ was effectively reproduced by the calculations including FSIs. The deuteron angular distribution exhibits a rather flat behavior, indicating that $\gamma d \to \pi^0\eta d$ is not expressed by the coherent sum of the elementary $\gamma N \to \pi^0\eta N$ amplitudes. Alternatively, a reaction sequence was considered to occur in $\gamma d \to \pi^0\eta d$. We successfully decomposed it into the $\pi^0\mathcal{D}_{01}$ and $\eta\mathcal{D}_{12}$ contributions by fitting them to the $d\sigma/dM_{\eta d}$ and $d\sigma/dM_{\pi d}$ data. Furthermore, we observed a clear peak corresponding to $\mathcal{D}_{01}$ in $d\sigma/dM_{\eta d}$. The mass of $\mathcal{D}_{01}$ was found to be $2.427^{+0.013}_{-0.006}$ GeV and the width was expressed by $\Gamma = \left(0.029^{+0.006}_{-0.029}\ \text{GeV}\right) + \left(0.00^{+0.41}_{-0.00}\right) p_\eta c$ for the momentum of η in the rest frame of ηd. According to the obtained parameters, $\mathcal{D}_{01}$ is expected to be the predicted bound state of ηd, or virtual state. Attraction between ηd is certainly very strong. In conclusion, coherent double neutral-meson photoproduction on the deuteron is a useful probe for studying a neutral meson and nucleus system. Further details are provided in Ref. [22].

Acknowledgments

The authors would like to convey their gratitude to the ELPH accelerator staff. They are also grateful to Mr. Ken'ichi Nanbu, Mr. Ikuro Nagasawa, and Mr. Kazue Matsuda for their technical support in the experiments. They also thank Prof. Alexander I. Fix, Prof. Bernd Krusche Prof. Mikhail Egorov, Prof. Heinz A Clement, Prof. Atsushi Hosaka, Prof. Kiyoshi Tanida, and Prof. Hiroyuki Fujioka for insightful discussions. This work was supported in part by JSPS KAKENHI Grant Numbers: 19002003, 17340063, 24244022, 26400287, 16H02188, 19H01902, 19H05141, 19H05181, and 21H00114.

1. S. Ajimura *et al.* (J-PARC E15 collaboration), *Phys. Lett. B* **789** (2019) 620.
2. T. Yamaga *et al.* (J-PARC E15 collaboration), *Phys. Rev. C* **102** (2020) 044002.
3. Q. Haider, and L.C. Liu, *Phys. Lett. B* **172** (1986) 257.
4. S.D. Bass, and A.W. Thomas, *Phys. Lett. B* **634** (2006) 368.
5. S. Hirenzaki, and H. Nagahiro, *Acta Phys. Polon. B* **45** (2014) 619.
6. S.D. Bass, and P. Moskal, *Rev. Mod. Phys.* **91** (2019) 015003.
7. D. Jido, H. Nagahiro, and S. Hirenzaki, *Phys. Rev. C* **66** (2002) 045202.
8. H. Nagahiro, D. Jido, and S. Hirenzaki, *Phys. Rev. C* **68** (2003) 035205.
9. H. Nagahiro, D. Jido, and S. Hirenzaki, *Nucl. Phys. A* **761** (2005) 92.
10. D. Jido, E.E. Kolomeitsev, H. Nagahiro, and S. Hirenzaki, *Nucl. Phys. A* **811** (2008) 158.
11. T. Ueda, *Phys. Rev. Lett.* **66** (1991) 297.
12. T. Ueda, *Phys. Lett. B* **291** (1992) 228.
13. S.A. Rakityansky *et al.*, *Phys. Rev. C* **53** (1996) 2043.
14. F. Plouin, P. Fleury, and C. Wilkin, *Phys. Rev. Lett.* **65** (1990) 690.

15. H. Calén *et al., Phys. Rev. Lett.* **79** (1997) 2642.
16. H. Calén *et al., Phys. Rev. Lett.* **80** (1998) 2069.
17. R. Bilger *et al., Phys. Rev. C* **69** (2004) 014003.
18. P. Hoffmann-Rothe *et al., Phys. Rev. Lett*. **78** (1997) 4697.
19. J. Weiß *et al., Eur. Phys. J. A* **11** (2001) 371.
20. T. Ishikawa *et al., Phys. Lett. B* **772** (2017) 398.
21. T. Ishikawa *et al., Phys. Lett. B* **789** (2019) 413.
22. T. Ishikawa *et al., Phys. Rev. C* **104** (2021) L052201.
23. T. Ishikawa *et al., JPS Conf. Proc.* **10** (2016) 031001.
24. H. Hama, *AAPPS Bulletin* **30** (2020) 41.
25. T. Ishikawa *et al., Nucl. Instrum. Meth. A* **622** (2010) 1.
26. F. Hinode *et al.,* in *Proceedings of 21st IEEE Particle Accelerator Conference* (PAC) (IEEE, Piscataway, 2005), pp. 2458-2460.
27. T. Ishikawa *et al., Nucl. Instrum. Meth. A* **811** (2016) 124.
28. Y. Matsumura *et al., Nucl. Instrum. Meth. A* **902** (2018) 103.
29. Y. Obara *et al., Nucl. Instrum. Meth. A* **922** (2019) 108.
30. H. Yamazaki *et al., ELPH Annual report* **2011-2013**, Tohoku University, (2014), p. 126.
31. T. Ishikawa *et al., Nucl. Instrum. Meth. A* **832** (2016) 108.
32. T. Ishikawa *et al., Nucl. Instrum. Meth. A* **694** (2012) 348.
33. T. Ishikawa *et al., Phys. Rev. C* **101** (2020) 052201 (R).
34. S. Agostineli *et al., Nucl. Instrum. Meth. A* **506** (2003) 250.
35. J. Allison *et al., IEEE Trans. Nucl. Sci.* **53** (2006) 270.
36. Geant4 website: `http://geant4.cern.ch/`.
37. A. Käser *et al., Phys. Lett. B* **748** (2015) 244.
38. M. Egorov, and A. Fix, *Phys. Rev. C* **88** (2013) 054611.
39. M. Egorov, *Phys. Rev. C* **101** (2020) 065205 .
40. S. Wycech and A.M. Green, *Phys. Rev. C* **64** (2001) 045206.
41. A. Fix and H. Arenhövel, *Eur. Phys. J. A* **9** (2000) 119.
42. H. Garcilazo, *Phys. Rev. C* **67** (2003) 067001.